

Scalar dispersion within a model canopy: Measurements and three-dimensional Lagrangian models

Daive Poggi^{a,b,c}, Gabriel Katul^{b,c,*}, John Albertson^{b,c}

^a *Dipartimento di Idraulica, Trasporti ed Infrastrutture Civili, Politecnico di Torino, Torino, Italy*

^b *Department of Civil and Environmental Engineering, Pratt School of Engineering, Duke University, Durham, NC 27708, USA*

^c *Nicholas School of the Environment and Earth Sciences, Duke University, Durham, NC, USA*

Received 28 December 2004; accepted 28 December 2004

Available online 15 July 2005

Abstract

Modeling scalar transport within canopies remains a vexing research problem in eco-hydrology and eco-hydraulics. Canopy turbulence is inhomogeneous, non-Gaussian, and highly dissipative, thereby posing unique challenges to three-dimensional Lagrangian Dispersion Models (LDM). Standard LDM approaches usually satisfy the well-mixed condition and account for turbulence inhomogeneity but not for its non-Gaussian statistics and enhanced dissipation. While numerous studies evaluated the importance of the former (with mixed results), few studies to date considered the latter. In this paper we present new data and explore: (1) the skill of LDM in reproducing mean scalar concentration distributions within dense and rigid canopies for source releases near the canopy top and near the ground, and (2) the extent to which these estimates are sensitive to the formulation of the mean turbulent kinetic energy dissipation rate (ϵ) profile. Toward this end, Laser Induced Florescence (LIF) and Laser Doppler Anemometry (LDA) were used to measure scalar concentration and Eulerian flow statistics within a dense model canopy in a rectangular flume. It is shown that LDM concentration predictions are sensitive to how ϵ is estimated. Good agreement between measured and modelled mean concentration distributions were obtained when ϵ was estimated from the mean squared longitudinal velocity gradients and isotropic turbulence principles. However, when ϵ was estimated from the widely used scaling arguments that employ a constant Lagrangian time scale (T_1) and a specified vertical velocity variance (σ_w^2) profile, the predicted concentrations diverged significantly from the LIF measurements. Better agreement was obtained when a constant mixing length scale was used with the σ_w^2 profile.

© 2005 Elsevier Ltd. All rights reserved.

Keywords: Canopy turbulence; Lagrangian dispersion models; Laser Doppler anemometry; Laser induced florescence; Inhomogeneous flows; Turbulent kinetic energy dissipation rate

1. Introduction

The transport of scalars (e.g. water vapor) within and above vegetation canopies continues to be a fundamental and practical research problem in eco-hydrology, eco-hydraulics, and biosphere–atmosphere exchange. For example, heat, water vapor, and CO₂ transport

from the soil–plant surface to the free atmosphere above the canopy [1,2] all require detailed parameterizations of turbulent transport processes within the canopy volume and across the canopy–atmosphere interface. One popular approach to modeling scalar transport within canopies is through the use of Lagrangian Dispersion Models (LDM) [3–11]. It is recognized that the application of LDM to canopy flows is complicated by several factors, including strong inhomogeneity, non-Gaussian flow statistics [12,13], and enhanced mean turbulent kinetic energy (TKE) dissipation rates (ϵ) within the canopy. Accounting for these factors in LDM while

* Corresponding author. Address: Nicholas School of the Environment and Earth Sciences, Box 90328, Duke University, Durham, NC 27708-0328, USA. Tel.: +1 919 613 8033; fax: +1 919 684 8741.

E-mail address: gaby@duke.edu (G. Katul).

satisfying the so-called well-mixed condition (*wmc*, i.e. an initially well mixed tracer remains well mixed) remains a subject of debate and extensive research.

There is broad acceptance that accounting for vertical inhomogeneity in the flow statistics is essential to modeling scalar dispersion in canopies [12,13]. This effect can be readily incorporated within LDM when the leaf area density profile is known, at least for the first and second moments of the flow statistics. Of the remaining two effects, the non-Gaussian flow statistics has received much more attention than has the dissipation rate formulation [14,4,15–21]. This may be attributed to the greater availability of measured velocity and scalar concentration moments than the availability of measured dissipation profiles. Despite the concentrated effort, the incorporation of non-Gaussian statistics has not unambiguously improved the predictive skills of LDM [18]. However, it has been shown that LDM concentration predictions for canopy sublayer (CSL) flows can be sensitive to how ϵ is specified [22].

Since field measurements of ϵ are complicated by numerous factors, LDM applications must rely on indirect estimates of the ϵ profile. However, there is no clear consensus on how to reliably estimate the ϵ profile inside plant canopies in terms of first and second moments of the flow field, at least as a reliable input to LDM approaches.

In this study we investigate how well a standard 3-D LDM reproduces measured concentration distributions using several popular formulations of the ϵ profile. We frame the study around laboratory measurements that employ source releases close to the bottom boundary (e.g. releases from the soil or litter), and source releases near the canopy top (e.g. deposition). Laser Induced Fluorescence (LIF) is used to measure the scalar concentration, and Laser Doppler Anemometry (LDA) is used to measure the Eulerian flow statistics. The goal of the analysis is a clear recommendation for robust estimation of ϵ profiles in LDM applications.

2. Experimental facilities

The experiment was conducted at the hydraulics Laboratory, DITIC Politecnico di Torino, in a recirculating constant head flume shown schematically in Fig. 1. The facility consists of a large rectangular channel 18 m long, 0.90 m wide, and 1 m deep. The channel walls are made of clear glass to allow the introduction of laser light through one side and collection of the scattered light on the other side. The canopy is placed in a test section 9 m long and 0.9 m wide situated 7 m downstream from the channel entrance. The canopy is composed of an array of vertical steel cylinders, 12 cm tall ($=h$), and 4 mm in diameter ($=d_r$) arranged in an aligned pattern with a density of 1072 rods m^{-2} . According to Poggi

et al. [23,24], such a density is dynamically equivalent to a dense canopy having an element area index (frontal area per unit volume) of 4.27 m^2 m^{-3} . The measured drag coefficient is comparable to drag coefficient estimates reported for dense forested ecosystems with leaf area index (LAI) ranging from 3.5 to 6.0 [25]. Measurements, described next, were conducted after the flow attained a uniform state at a water depth ($=h_w$) of 60 cm.

2.1. Velocity measurements

The velocity was measured by two-component LDA in forward scattering mode. A key advantage of LDA is its non-intrusive nature, its small averaging volume, and its ability to measure velocity close to embedded objects such as the model canopy. Further details about the LDA configuration and signal processing can be found in Poggi et al. [26,27]. With the LDA, a measurement run consists of sampling time series of the longitudinal and vertical velocity component, u and w respectively, at a particular spatial position. The sampling location was chosen such that the measured local temporal statistics were representative of the horizontally-averaged temporal statistics, following an analysis of the more spatially expansive data for the model canopy [23,28]. We sampled the entire depth of the boundary layer at 1 cm vertical increments with 30 runs. The sampling duration and frequency were 3600 s per run at 2500–3000 Hz. The bulk Reynolds number, Re_b , calculated using the vertically-averaged velocity (U_b) across the water depth, h_w , is 116,000 which ensures fully-developed turbulence.

2.2. Scalar concentration measurements

The planar LIF technique was employed to measure the local instantaneous dye concentration in the flow. This technique is based on the capacity of certain dye to react with fluorescence when excited by a laser sheet. The concentration measurements were conducted by injecting two types of fluorescent dye solution, Fluorescein and Rhodamine 6G, through slits (less than 0.3 mm thick) at the bottom ($z/h = 0.05$) and at the canopy top ($z/h = 1.05$), respectively. The light source was a 300 mW continuous fixed wavelength ion-argon laser (Melles Griot mod. 543-A-A03). A lens system was used to provide a 0.6 mm thick light sheet of about 60 cm in height and 25 cm in width. When excited by the laser, the Fluorescein and Rhodamine 6G emit a metallic green and a bright red light, respectively.

Image sequences were recorded for an area in the x – z plane centered in the middle of the channel starting from the ground up to $3h$ and having a width of $4h$ (longitudinal) with a color CCD video camera. This video set-up allowed us to acquire digital movies with high resolution (720×480 pixels corresponding to a resolution of

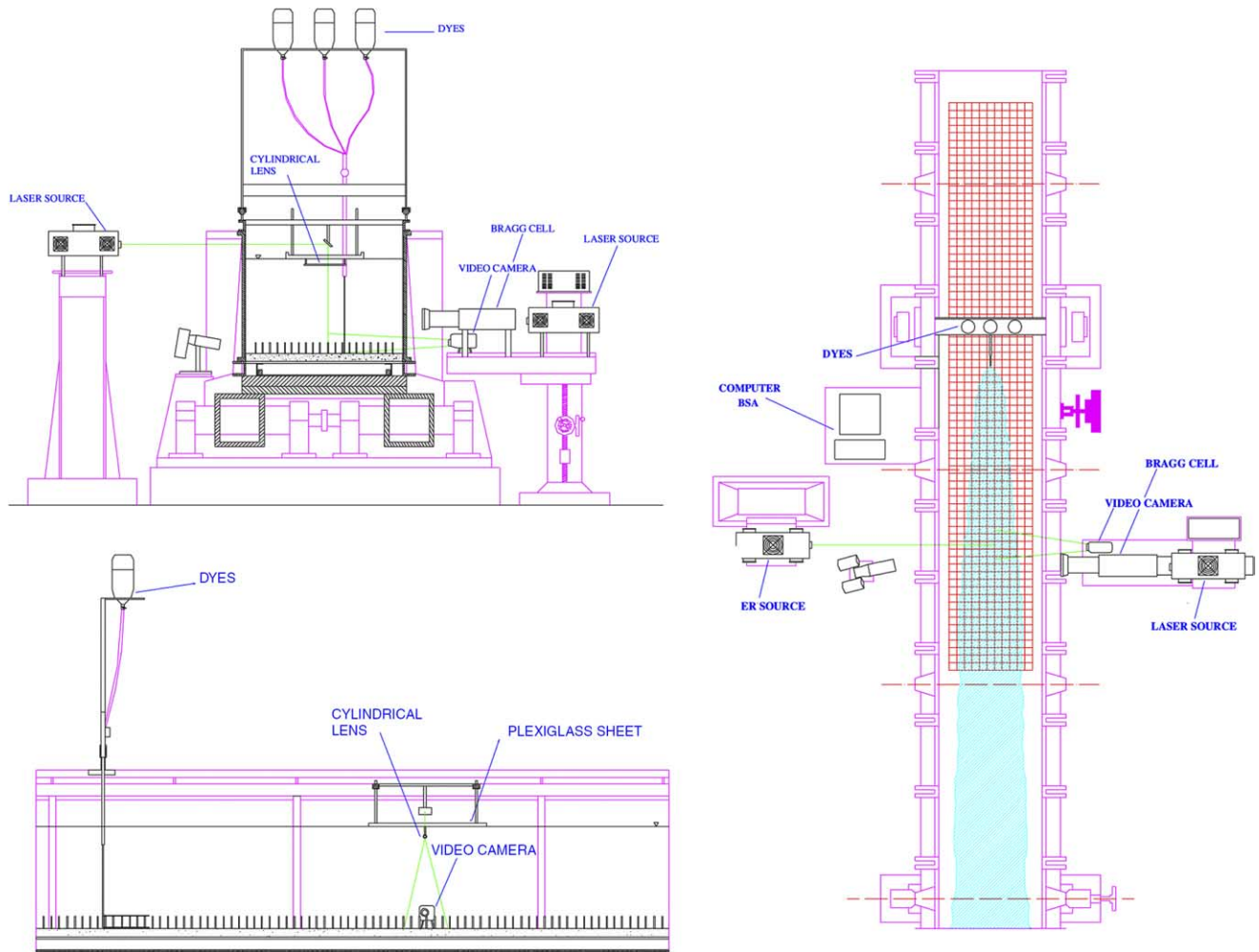


Fig. 1. Plan and lateral view of the channel flow facility, the Laser Doppler Anemometry (LDA) setup, and the laser induced fluorescence (LIF) setup. The dye injection is conducted at $z/h = 0.05$ and 1.05 .

0.5 mm, DV-AVI with NTSC format and high frequency of 30 frames per second). A 12 min video sequence was used to compute the scalar concentration statistics for the two source releases. A relationship between the intensity level of the emitted light and the mean concentration was developed empirically. Four solutions with different known concentrations C for each dye were prepared in a small square tank. For each dye concentration, a short video of the light intensity was recorded and analyzed. In our case, the dye concentration was far from the saturation limit, such that the dye concentration was linearly dependent on the strength of the remitted light.

3. Theory

Among the various three-dimensional LDM approaches proposed over the past two decades, the Thomson [29] and Pope [30,31] frameworks are now widely used. Both of these models satisfy the *wmc* for

strongly inhomogeneous flows. We will focus on [29] model, as it is particularly popular in atmospheric sub-layer (ASL) and mixed layer (ML) turbulence applications. Its popularity is largely due to it only requiring first and second moments of the Eulerian velocity field, which can be measured or readily estimated from similarity theory [32], making it relatively simple to implement [9,33]. While much of the theory is already presented in Rodean [32] and Reynolds [8], a review of the Thomson [29] model is provided for completeness.

The trajectory of a single fluid element is given by

$$x_i(t + \Delta t) = x_i(t) + \int_t^{t+\Delta t} (u_i) dt, \quad (1)$$

where u_i is the instantaneous fluid element velocity along direction x_i , Δt is the discrete simulation time interval, and t is time. The subscripts i, j, k are used throughout to denote components of Cartesian tensors. Per the original model of Thomson [29], the evolution of a tracer particle's velocity is taken as a continuous Markov pro-

cess. Following this assumption, the evolution of u_i can be expressed by

$$du_i = a_i(x_k, u_k, t) dt + b(x_k, u_k, t) d\Omega_i, \quad (2)$$

where a_i are the drift coefficients, b is the random acceleration coefficient, and $d\Omega$ is a Gaussian random variable with zero mean and variance dt . The function b ($= \sqrt{C_0\epsilon}$) is determined by requiring that the Lagrangian velocity structure function in the inertial subrange satisfies Kolmogorov's similarity theory [34]. We note here that Eulerian structure function measurements within the canopy significantly depart from Kolmogorov scaling [35,23] thereby introducing additional (and less appreciated) uncertainty in the Thomson [29] formulation for these canopy sublayer applications. For two- and three-dimensional turbulence Thomson [29] showed that the drift term, a_i , can be constrained but not completely determined by requiring consistency with prescribed Eulerian velocity statistics. Adopting the criterium of the simplest choice [29], and after some algebra, the model in three dimensions becomes [32]

$$du'_1 = \left[-\frac{C_0\epsilon}{2}(\lambda_{11}u'_1 + \lambda_{13}u'_3) + \frac{\partial \bar{u}_1}{\partial x_3}u'_3 + \frac{1}{2} \frac{\partial \overline{u'_1 u'_3}}{\partial x_3} \right] dt + \left[\frac{\partial \overline{u'_1 u'_1}}{\partial x_3}(\lambda_{11}u'_1 + \lambda_{13}u'_3) + \frac{\partial \overline{u'_1 u'_3}}{\partial x_3}(\lambda_{13}u'_1 + \lambda_{33}u'_3) \right] \frac{u'_3}{2} dt + \sqrt{C_0\epsilon} d\Omega, \quad (3)$$

$$du'_2 = \left[\left(-\frac{C_0\epsilon}{2} + \frac{1}{2} \frac{\partial \overline{u'_2 u'_2}}{\partial x_3} \right) (\lambda_{22}u'_2) \right] dt + \sqrt{C_0\epsilon} d\Omega, \quad (4)$$

$$du'_3 = \left[-\frac{C_0\epsilon}{2}(\lambda_{13}u'_1 + \lambda_{33}u'_3) + \frac{1}{2} \frac{\partial \overline{u'_3 u'_3}}{\partial x_3} \right] dt + \left[\frac{\partial \overline{u'_1 u'_3}}{\partial x_3}(\lambda_{11}u'_1 + \lambda_{13}u'_3) + \frac{\partial \overline{u'_3 u'_3}}{\partial x_3}(\lambda_{13}u'_1 + \lambda_{33}u'_3) \right] \frac{u'_3}{2} dt + \sqrt{C_0\epsilon} d\Omega, \quad (5)$$

where the overbar denotes time averaging, u'_i are the (instantaneous) turbulent velocities at position x_i and time t , C_0 (≈ 5.5) is a similarity constant (related to the Kolmogorov constant) that is a subject of some debate [36,37], and the λ 's, can be related to the Eulerian flow statistics using

$$\lambda_{11} = \left(\overline{u'_1 u'_1} - \frac{(\overline{u'_1 u'_3})^2}{\overline{u'_3 u'_3}} \right)^{-1}, \quad (6)$$

$$\lambda_{22} = \frac{1}{\overline{u'_2 u'_2}}, \quad (7)$$

$$\lambda_{33} = \left(\overline{u'_3 u'_3} - \frac{(\overline{u'_1 u'_3})^2}{\overline{u'_1 u'_1}} \right)^{-1}, \quad (8)$$

$$\lambda_{13} = \left(\overline{u'_1 u'_3} - \frac{(\overline{u'_1 u'_1})(\overline{u'_3 u'_3})}{\overline{u'_1 u'_1} \overline{u'_3 u'_3}} \right)^{-1}, \quad (9)$$

where $\overline{u'_1 u'_1}$ ($= \sigma_u^2$), $\overline{u'_2 u'_2}$ ($= \sigma_v^2$), $\overline{u'_3 u'_3}$ ($= \sigma_w^2$) are the Eulerian variances of the three velocity components, and $\overline{u'_1 u'_3}$ ($= \overline{u'w'}$) is the Reynolds stress.

The first and second moments of the velocity components can be measured or accurately computed within the canopy; however, measuring and modeling ϵ continues to be a fundamental challenge within plant canopies. The most common dissipation estimate (for applications such as this) is

$$\epsilon = \frac{2\overline{u'_3 u'_3}}{C_0 \times T_1}, \quad (10)$$

where T_1 is the Lagrangian integral time scale. Unfortunately, T_1 is difficult (if not impossible) to measure directly and remains a source of uncertainty in the application of LDM to canopy flows. One approach is to assume that the measured integral time scale for vertical velocity (I_w) approximates well T_1 [12]. The advantage of this method is that I_w can be readily measured from vertical velocity time series in the field. Hence, with this approximation for T_1 , we define

$$\epsilon_{I_w} = \frac{2\overline{u'_3 u'_3}}{C_0 \times I_w}. \quad (11)$$

While the profile of I_w can be measured, it is rare that field experiments routinely monitor such a quantity at several levels within the canopy. Hence, an additional simplification is to a priori specify the shape of I_w within the CSL (and ASL). According to Raupach [12], when I_w is normalized by h/u_* , data sets from a wide range of canopies approximately collapse to a typical Eulerian time scale profile T_{EU} given by

$$T_{EU} = \begin{cases} \beta \frac{h}{u_*}; & \frac{z}{h} < 2, \\ \frac{k_v(z-d)u_*}{\sigma_w^2}; & \frac{z}{h} > 2, \end{cases}$$

where $\beta = 0.3$, d is the zero-plane displacement height ($\approx 2/3h$), k_v is the von Karman constant ($=0.4$), and $u_* = [-\overline{u'w'}]^{1/2}$ is the friction velocity defined at $z/h = 1$ [35]. The dissipation rate estimated by setting T_1 to T_{EU} is given by

$$\epsilon_{EU} = \frac{2\overline{u'_3 u'_3}}{C_0 \times T_{EU}}. \quad (12)$$

Finally, when longitudinal velocity time series is sampled at sufficiently high frequency to resolve the dissipation spectrum, ϵ can be estimated from the homogeneous and isotropic relationship [38]

$$\epsilon_{\text{iso}} = 15\nu \overline{\left(\frac{\partial u'_1}{\partial x_1}\right)^2}, \quad (13)$$

where the spatial derivative is approximated from the temporal derivative using Taylor's frozen turbulence hypothesis, and ν is the kinematic viscosity. This method is well-suited to LDA measurements as the sampling frequency is sufficiently high to resolve the viscous dissipation frequency range. We refer to ϵ_{iso} as the "measured" dissipation given that it makes no assumption about the Lagrangian time scale or power-law scaling within the inertial subrange. Strictly speaking, ϵ is not measured by ϵ_{iso} though ϵ_{iso} does represent our best estimate of the true ϵ from one-dimensional time series of u as we show later using the TKE budget.

We will compare the measured and the LDM predicted concentration for all three estimates ($\epsilon (= \epsilon_{\text{iso}}, \epsilon_{I_w}$ and ϵ_{EU}) to assess the overall sensitivity of LDM to the ϵ formulation.

4. Results

We briefly describe the measured Eulerian flow statistics and scalar concentration distribution within and near the canopy top. Then, we proceed to discuss the skill of LDM in reproducing measured relative concen-

tration distributions for source releases at $z/h = 1.05$ and $z/h = 0.05$ using ϵ_{iso} , ϵ_{I_w} , and ϵ_{EU} .

4.1. Eulerian velocity moments

Fig. 2 shows the measured velocity statistics obtained from the LDA within and above the canopy. For $z/h < 2$, the rapid attenuation of the mean velocity and Reynolds stress profiles compare well with numerous velocity measurements collected in forested canopies, agricultural crops, and dense rods within wind tunnels [35] suggesting that the present experiment represents reasonably well canopy turbulence in the field. Also, the range of values in skewness (sk) and kurtosis factors (ku) are consistent with numerous CSL field experiments.

Fig. 3 compares the profiles of ϵ_{iso} with ϵ_{EU} and ϵ_{I_w} . All three estimates suggest that ϵ is highly inhomogeneous and non-monotonic within the canopy. However, the disagreement between these estimates is large (more than a factor of 4 for certain z/h within the canopy) and will significantly impact the skill of LDM concentration predictions. We also compared how well these three formulations compare with the dissipation rate estimated as a residual from the TKE budget (henceforth referred to as P_d) given by

$$P_d = -P_s + P_w + P_t, \quad (14)$$

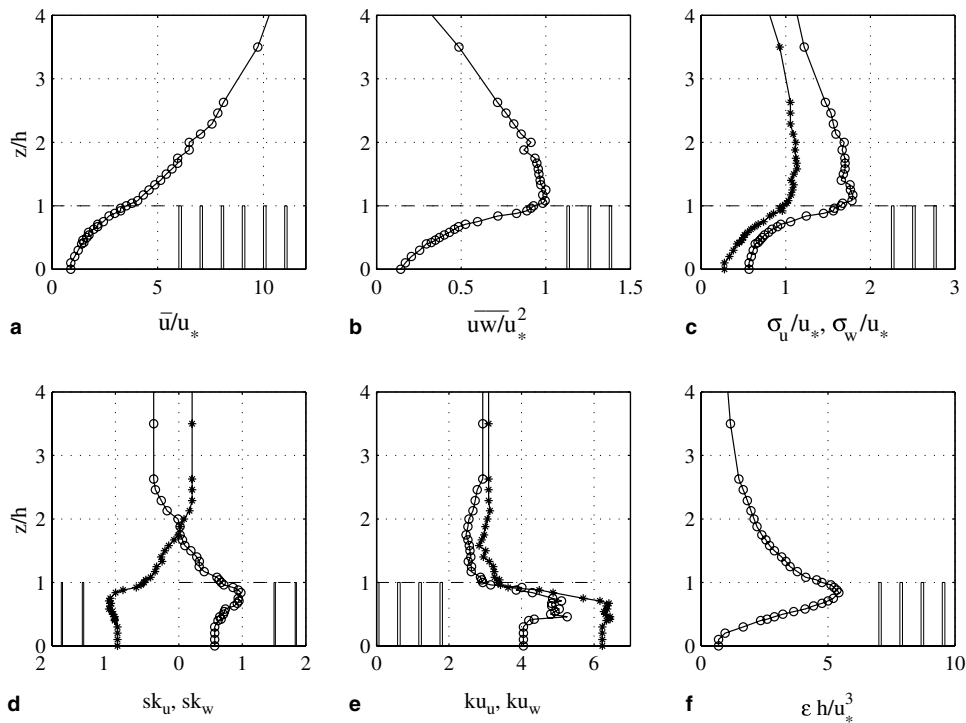


Fig. 2. Variation of temporally- and horizontally-averaged velocity statistics with normalized height (z/h) for (a) mean longitudinal velocity \bar{u}/u_* , (b) mean shear stress \overline{uw}/u_*^2 , (c) longitudinal (open circles) and vertical (stars) velocity standard deviations $\sigma_u = \overline{u'^2}/u_*$ and $\sigma_w = \overline{w'^2}/u_*$, respectively, (d) longitudinal (open circles) and vertical (stars) velocity skewness $sk_u = \overline{u'^3}/\sigma_u^3$ and $sk_w = \overline{w'^3}/\sigma_w^3$, respectively, and (e) longitudinal (open circles) and vertical (stars) velocity kurtosis $ku_u = \overline{u'^4}/\sigma_u^4$ and $ku_w = \overline{w'^4}/\sigma_w^4$, respectively, and (f) the normalized mean turbulent kinetic energy $\epsilon_{\text{iso}}h/u_*^3$ is added for reference.

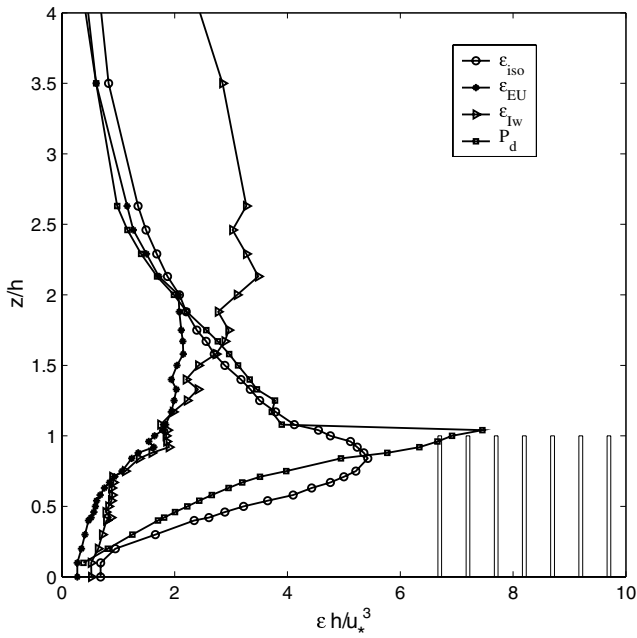


Fig. 3. Comparison between the three dissipation rate profiles: ϵ_{iso} (open circles), ϵ_{EU} (asterisk), and ϵ_{Iw} (triangle). For reference, the dissipation rate determined as a residual from the TKE budget is also shown (squares).

where P_s , P_w , P_t , and are the shear production, wake production, and turbulent transport, respectively, and are independently estimated from the measured velocity statistics using the formulations in [28]. Deep within the canopy, while ϵ_{iso} is in agreement with P_d , the magnitude of ϵ_{EU} and ϵ_{Iw} are significantly lower. The largest departure between P_d and ϵ_{iso} , is near the canopy top, though the apparent strong discontinuity in P_d in this region is attributed to approximations in the evaluation of the three terms in Eq. (14) as discussed in [28]. Well above the canopy ($z/h > 2$), ϵ_{iso} and ϵ_{EU} collapse to P_s ($=P_d$) suggesting some equilibrium between TKE production and dissipation, though ϵ_{Iw} does not. The disagreement between ϵ_{Iw} and P_s is perhaps due to the sensitivity of I_w to oscillations in the free water surface for $z/h > 2$. In short, the comparisons in Fig. 3 lend support to the use of ϵ_{iso} as the best estimate of the dissipation rate profile for LDM models given their consistency with the TKE budget.

4.2. Concentration measurements

Fig. 4a and b display the normalized time-averaged concentration ($\hat{C} = C/C_*$) as measured by LIF in the $x-z$ plane for the two scalar source releases, where $C_* = \int_0^{5h} C(z) dz$. It is clear from these two figures that the time-averaged concentration is approximately

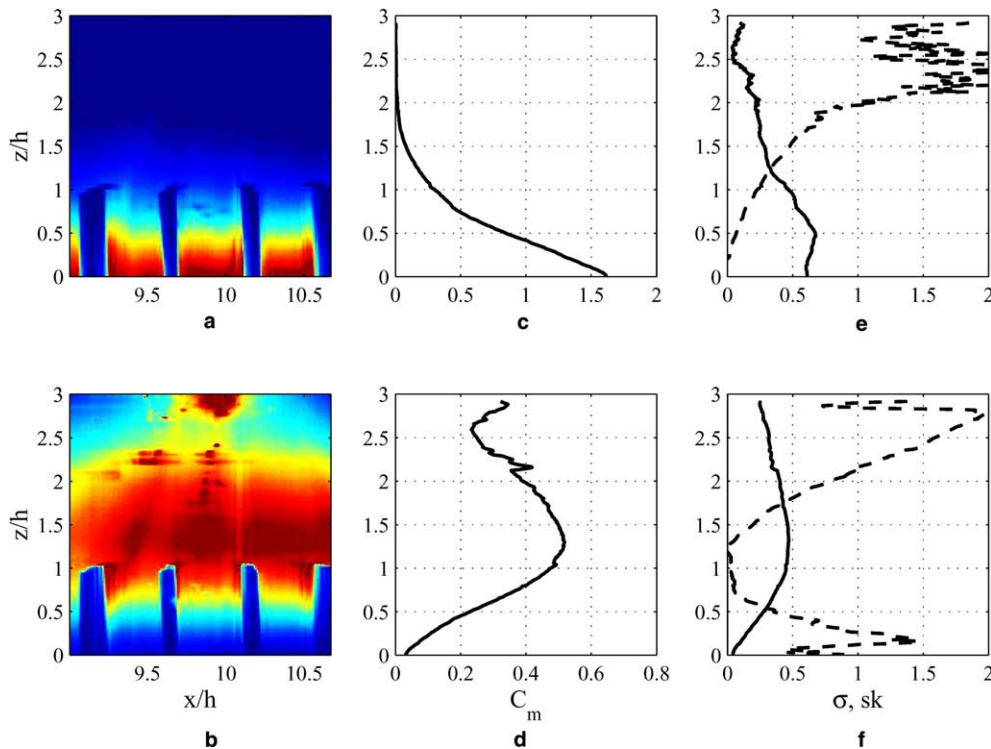


Fig. 4. (a) Time-averaged concentration as measured by LIF in the $x-z$ plane for the scalar source release at $z/h = 1.05$, (b) Same as (a) but for scalar source release at $z/h = 0.05$, (c) time and horizontally-averaged concentration profile for $x/h \in [9.5-10.5]$ and for source release at $z/h = 0.05$, (d) Same as (c) but for source release at $z/h = 1.05$. (e) and (f) show the time and horizontally-averaged variance and skewness profiles around the mean profiles in (c) and (d), respectively.

planar homogeneous for $x/h \in [9.5-10.5]$ but strongly inhomogeneous in the vertical. Fig. 4c and d show the time- and horizontally-averaged concentration (C_m) profiles along $x/h \in [9.5-10.5]$ for the two source releases. These two profiles serve as the measured concentration profiles for which the LDM calculations will be compared against. We also report in Fig. 4e and f the time- and horizontally-averaged variance and skewness profiles around the mean concentration profile shown in Fig. 4c and d. It is clear that the higher order concentration statistics are non-Gaussian in direct violation of LDM assumptions.

4.3. Comparison between model calculations and measurements

The LDM model computes the concentration as follows: (1) the source is modelled with 20,000 individual fluid particles, (2) the trajectories are computed at $dt = 0.01I_w$, and (3) a reflection boundary at the base of the flume ($z/h = 0$) along with an absorbing boundary at the free water surface profile ($z/h = 5$) are specified. We note that describing a boundary condition at the free water surface is not trivial; however, based on the flow visualizations for both source releases, the dye never reached the free water surface at $x/h = 10$. We extrapolated the measured Eulerian flow statistics in Fig. 2 to $z/h = 0$ using standard boundary layer similarity and in a manner to ensure local homogeneity so as to satisfy the well-mixed condition near the ground as discussed in Wilson and Flesch [39] and Rodean [32]. The C_m for the three estimates of ϵ in Fig. 3 and for the two source locations are compared with the LIF measured C_m in Figs. 5 and 6. Adding the constraints suggested by Reynolds [9] and Thomson [29] on the minimum dt did not change the concentration profiles by more than 3% in Figs. 5 and 6. The theoretical upper limit on dt discussed in Wilson and Zhuang [40] is satisfied at all points in the flow domain.

For both scalar releases, it is clear that the agreement between measured and modeled C_m is superior for $\epsilon = \epsilon_{iso}$, when compared to the other two dissipation profile estimates, at least in terms of regression statistics and minimum rmse (see Table 1). A logical question then is whether ϵ_{iso} can be estimated using some characteristic time or length scale along with second order moments of the velocity statistics, discussed next.

4.4. Estimating the dissipation rate profile from length and time scales

As stated earlier, the approach taken in classical LDM is to assume that the Lagrangian time scale is constant within the CSL, which implies that all the vertical variability in ϵ can be explained by the vertical variations in σ_w^2 . However, the dissipation rate inside the can-

opy may require a height-dependent Lagrangian time scale.

One practical and plausible alternative to a constant time scale is a constant mixing length scale within the canopy. A height-dependent characteristic velocity can then be used to obtain a variable time scale that preserves ϵ_{iso} . Constant mixing length scales have already been assumed and used in numerous second order clo-

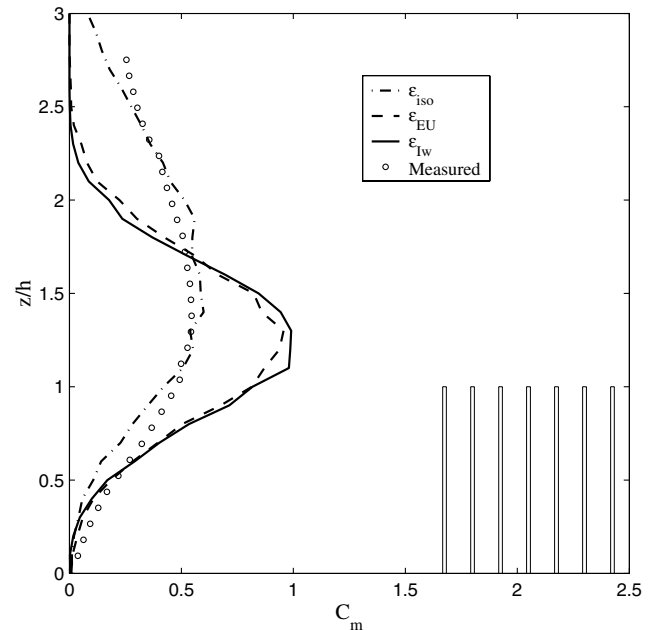


Fig. 5. Comparison between measured (open circles) and modelled relative concentration with normalized height (z/h) for scalar source releases at $z/h = 1.05$ and for the three dissipation profiles in Fig. 3.

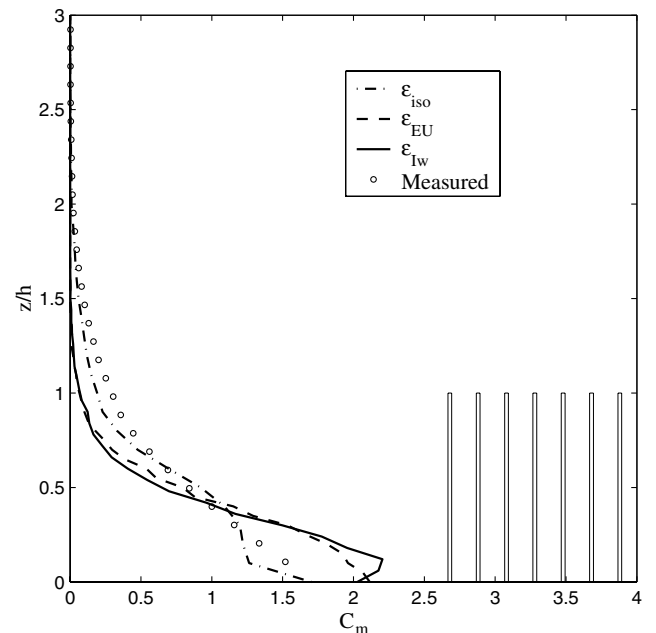


Fig. 6. Same as Fig. 5 but for scalar source release at $z/h = 0.05$ and for the three dissipation profiles in Fig. 3.

Table 1
Comparison between measured and modeled normalized time-averaged concentration, \hat{C}

	Source releases $z/h = 1.05$			Source releases $z/h = 0.05$		
	ϵ_{iso}	ϵ_{EU}	ϵ_{I_w}	ϵ_{iso}	ϵ_{EU}	ϵ_{I_w}
<i>A</i>	0.78	0.34	0.30	0.94	0.82	0.88
<i>B</i>	0.08	0.24	0.26	0.03	0.08	0.08
rmse	0.03	0.10	0.11	0.04	0.11	0.12
<i>R</i>	0.97	0.75	0.73	0.99	0.94	0.93

The regression model is of the form $y = Ax + B$, where y is the modeled and x is the measured \hat{C} . The root-mean square error (rmse) and the correlation coefficient *R* are also shown.

sure model calculations [41,42,25,43] with reasonable success in reproducing first and second moments of the velocity field. Based on Poggi et al. [23], we assume that the mixing length scale is constant ($=\beta'h$) inside the canopy and varies linearly above. After experimenting with different velocity scales (e.g. \bar{u}_1 , $k^{0.5}$, u_* , and σ_w) to obtain a dissipation time scale, we found that

$$T_{EU} = \begin{cases} \frac{\beta'h}{\sigma_w}; & \frac{z}{h} < d + \frac{\alpha h}{k_v}, \\ \frac{k_v(z-d)u_*}{\sigma_w^2}; & \frac{z}{h} > d + \frac{\alpha h}{k_v}, \end{cases}$$

best represents $2\sigma_w^2/(C_0\epsilon_{iso})$, which is consistent with the Lagrangian time scale model in Massman and Weil [42]. The magnitude of the difference between the various time scale estimates are shown in Fig. 7. It is clear that within the canopy, τ_{EU} matches well the variability in $2\sigma_w^2/(C_0\epsilon_{iso})$ for $\beta' = 0.05$. However, this estimate of β' cannot be constant but must vary with the rod density and diameter (for high Reynolds numbers). From field

experiments, Massman and Weil [42] and Sanz [44] suggested that

$$\beta' = \frac{\alpha}{hC_d a_d}, \tag{15}$$

where α appears to be constant (≈ 0.06) for a wide range of canopies, C_d is the drag coefficient, and a_d is the mean leaf area density. Hence, to account for differences in leaf area density and drag coefficients on β' , the above formulation may be used with $a_d = LAI/h$, where LAI is the leaf area index. That is,

$$\beta' \simeq \frac{\alpha}{C_d \times LAI}. \tag{16}$$

Using the above formulation for this flume setup, the depth-averaged drag coefficient is about 0.3 and the equivalent LAI is about 4 as shown in Poggi et al. [23], resulting in an approximate $\beta' = 0.05$ which is consistent with the β' in Fig. 7.

5. Conclusions

Through detailed experiments and Lagrangian model simulations, we evaluated the applicability of the Thomson [29] approach to canopy turbulence using three dissipation formulations. All the Eulerian velocity statistics needed to drive the Thomson [29] model were measured by LDA or independently estimated. The Thomson [29] model does not consider non-Gaussian turbulence and intermittency, both are defining features of canopy turbulence. However, the Thomson [29] model explicitly considers the inhomogeneity in the flow in a manner consistent with the well-mixed condition. Despite its simplifications, we found that LDM predicted and measured LIF concentration distribution within the canopy are in good agreement but the modelled concentration values are sensitive to the prescribed mean turbulent kinetic energy dissipation rate profile. The agreement between model calculations and measurements were best when the measured dissipation rate was used instead of modelled estimates based on constant Lagrangian time scales and vertical velocity variance profile. This good agreement indirectly supports the working hypothesis of Flesch and Wilson [18] who argued that while the turbulence in plant canopies is strongly non-Gaussian,

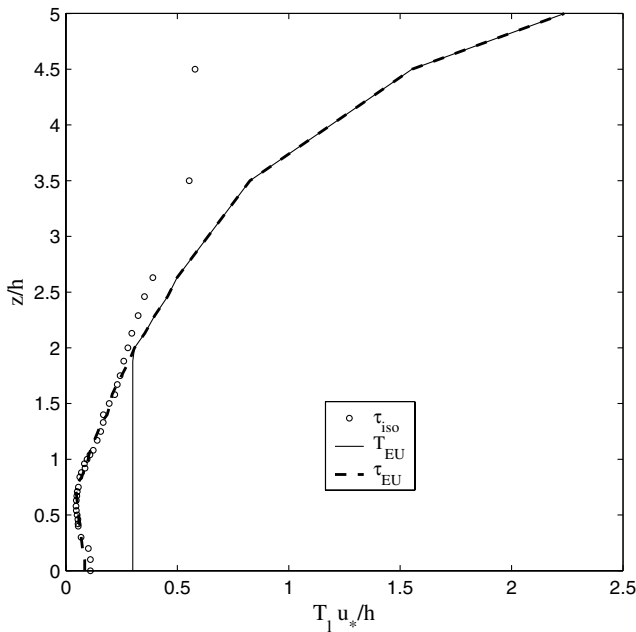


Fig. 7. Variation of T_1 estimated from τ_{iso} (circles), T_{EU} (solid line), and τ_{EU} (dashed line) with z/h . All three time scale estimates are normalized with u_*/h .

the higher order velocity moments are of secondary importance in determining the mean concentration when compared to the effects of the strong vertical gradients in the Reynolds stress tensor.

We also investigated two possible formulations for the turbulent kinetic energy dissipation rate profiles inside canopies. The first is the standard approach which assumes that the Lagrangian time scale is constant, while the second assumes that the mixing length scale is constant. We showed that the constant mixing length scale, in combination with the vertical velocity variance, better reproduces the measured dissipation rate profile when compared to the constant Lagrangian time scale method.

The broad impact of this work is perhaps best placed in the context of Lumley's [45] statement about the state of turbulence models. "*In our present state of understanding, these simple models will always be based in part on good physics, in part, on bad physics, and in part, on shameless phenomenology.*" Demonstrating how sensitive the LDM computed concentration is to "bad physics" and "shameless phenomenology" is necessary (but not sufficient) toward building robust and accurate formulations for canopy turbulence that can then be used in problems pertaining to scalar production and transport inside canopies. This work showed that accounting for the inhomogeneity in the flow field and properly parameterizing the mean dissipation rate profile are sufficient to reproduce the inhomogeneity in the mean concentration distribution using standard LDM despite their Gaussian turbulence assumption, and the documented non-Gaussianity in velocity and scalar measurements.

Acknowledgements

The first author acknowledges support for the flume experiments from the Dipartimento di Idraulica, Trasporti ed Infrastrutture Civili, Politecnico di Torino, Torino, Italy. The second and third authors acknowledge support from the Center on Global Change (Duke University) during their fall of 2002 leave. Funding was provided by the National Science Foundation (NSF-EAR and NSF-DMS), the Biological and Environmental Research (BER) Program, U.S. Department of Energy, through the Southeast Regional Center (SERC) of the National Institute for Global Environmental Change (NIGEC), and through the Terrestrial Carbon Processes Program (TCP).

References

- [1] Baldocchi D. A Lagrangian random-walk model for simulating water-vapor, CO₂ and sensible heat-flux densities and scalar profiles over and within a soybean canopy. *Bound-Lay Meteorol* 1992;61:113–44.
- [2] Scanlon T, Albertson J. Turbulent transport of carbon dioxide and water vapor within a vegetation canopy during unstable conditions: identification of episodes using wavelet analysis. *J Geophys Res* 2001;106:7251–62.
- [3] Raupach M. Applying Lagrangian fluid-mechanics to infer scalar source distributions from concentration profiles in plant canopies. *Agr Forest Meteorol* 1989;47:85–108.
- [4] Luhar A, Britter R. A random-walk model for dispersion in inhomogeneous turbulence in a convective boundary-layer. *Atmos Environ* 1989;23:1911–24.
- [5] Luhar A, Rao K. Lagrangian stochastic dispersion model simulations of tracer data in nocturnal flows over complex terrain. *Atmos Environ* 1994;28:3417–31.
- [6] Wilson J, Sawford B. Review of Lagrangian stochastic models for trajectories in the turbulent atmosphere. *Bound-Lay Meteorol* 1996;78:191–210.
- [7] Hsieh C, Katul G, Schieldge J, Sigmon J, Knoerr K. The Lagrangian stochastic model for fetch and latent heat flux estimation above uniform and nonuniform terrain. *Water Resour Res* 1997;33:427–38.
- [8] Reynolds A. A Lagrangian stochastic model for particle trajectories in non-Gaussian turbulent flows. *Fluid Dyn Res* 1997;19:277–88.
- [9] Reynolds A. On the formulation of Lagrangian stochastic models of scalar dispersion within plant canopies. *Bound-Lay Meteorol* 1998;86:333–44.
- [10] Schmid H. Footprint modeling for vegetation atmosphere exchange studies: a review and perspective. *Agr Forest Meteorol* 2002;113:159–83.
- [11] Cassiani M, Giostra U. A simple and fast model to compute concentration moments in a convective boundary layer. *Atmos Environ* 2002;36:4717–24.
- [12] Raupach M. A practical Lagrangian method for relating scalar concentrations to source distributions in vegetation canopies. *Quart J Roy Meteorol Soc* 1989;115:609–32.
- [13] Sawford B. Recent developments in the Lagrangian stochastic-theory of turbulent dispersion. *Bound-Lay Meteorol* 1993;62:197–215.
- [14] Legg B. Turbulent dispersion from an elevated line source—Markov-chain simulations of concentration and flux profiles. *Quart J Roy Meteorol Soc* 1983;109:645–60.
- [15] Kaplan H, Dinar N. A stochastic-model for the dispersion of a nonpassive scalar in a turbulent field. *Atmos Environ Part-A* 1992;26:2413–23.
- [16] Kaplan H, Dinar N. A 3-dimensional model for calculating the concentration distribution in inhomogeneous turbulence. *Bound-Lay Meteorol* 1993;62:217–45.
- [17] Tampieri F, Scarani C, Giostra U, Brusasca G, Tinarelli G, Anfossi D, et al. On the application of random flight dispersion models in inhomogeneous turbulent flows. *Ann Geophys* 1992;10:749–58.
- [18] Flesch T, Wilson J. A 2-dimensional trajectory-simulation model for non-Gaussian, inhomogeneous turbulence within plant canopies. *Bound-Lay Meteorol* 1992;61:349–74.
- [19] Du S, Wilson J, Yee E. On the moments approximation method for constructing a Lagrangian stochastic-model. *Bound-Lay Meteorol* 1994;70:273–92.
- [20] Du S, Wilson J, Yee E. Probability density-functions for velocity in the convective boundary-layer, and implied trajectory models. *Atmos Environ* 1994;28:1211–7.
- [21] Maurizi A, Tampieri F. Velocity probability density functions in Lagrangian dispersion models for inhomogeneous turbulence. *Atmos Environ* 1999;33:281–9.
- [22] Rannik U, Markkanen T, Raittila J, Hari P, Vesala T. Turbulence statistics inside and over forest: influence on footprint prediction. *Bound-Lay Meteorol* 2003;109:163–89.

- [23] Poggi D, Porporato A, Ridolfi L, Katul G, Albertson J. The effect of vegetation density on canopy sublayer turbulence. *Bound-Lay Meteorol* 2004;111(3):565–87.
- [24] Poggi D, Katul G, Albertson J. A note on the contribution of dispersive fluxes to momentum transfer within canopies. *Bound-Lay Meteorol* 2004;111(3):615–21.
- [25] Katul G, Albertson J. An investigation of higher-order closure models for a forested canopy. *Bound-Lay Meteorol* 1998;89:47–74.
- [26] Poggi D, Porporato A, Ridolfi L. An experimental contribution to near-wall measurements by means of a special laser Doppler anemometry technique. *Exp Fluids* 2002;32:366–75.
- [27] Poggi D, Porporato A, Ridolfi L. Analysis of the small-scale structure of turbulence on smooth and rough walls. *Phys Fluids* 2003;15:35–46.
- [28] Poggi D, Katul G, Albertson J. Momentum transfer and turbulent kinetic energy budgets within a dense model canopy. *Bound-Lay Meteorol* 2004;111(3):589–614.
- [29] Thomson D. Criteria for the selection of stochastic-models of particle trajectories in turbulent flows. *J Fluid Mech* 1987;180:529–56.
- [30] Pope S. Lagrangian pdf methods for turbulent flows. *Ann Rev Fluid Mech* 1994;26:23–63.
- [31] Pope S. Stochastic Lagrangian models of velocity in homogeneous turbulent shear flow. *Phys Fluids* 2002;14:1696–702.
- [32] Rodean H. Stochastic Lagrangian models of turbulent diffusion. *Meteorological monographs*, vol. 26, No. 48. Boston, MA: American Meteorological Society; 1996.
- [33] Sawford B. Rotation of trajectories in Lagrangian stochastic models of turbulent dispersion. *Bound-Lay Meteorol* 1999;93:411–24.
- [34] Kolmogorov AN. The local structure of turbulence in incompressible viscous fluid for very large Reynolds number. *Dokl Akad Nauk SSSR* 1941;30:299–304.
- [35] Finnigan J. Turbulence in plant canopies. *Ann Rev Fluid Mech* 2000;32:519–71.
- [36] Reynolds A. Comments on the universality of the Lagrangian velocity structure function constant c_0 across different kinds of turbulence. *Bound-Lay Meteorol* 1998;89:161–70.
- [37] Du S. Universality of the Lagrangian velocity structure function constant (C_0) across different kinds of turbulence. *Bound-Lay Meteorol* 1997;83:207–19.
- [38] Tennekes H, Lumley J. *A first course in turbulence*, vol. I. Cambridge, MA: MIT Press; 1972.
- [39] Wilson J, Flesch T. Flow boundaries in random-flight dispersion models—enforcing the well-mixed condition. *J Appl Meteorol* 1993;32:1695–707.
- [40] Wilson J, Zhuang Y. Restriction on the timestep to be used in stochastic Lagrangian models of turbulent dispersion. *Bound-Lay Meteorol* 1989;49:309–16.
- [41] Wilson N, Shaw R. A higher order closure model for canopy flow. *J Appl Meteorol* 1977;16:1198–205.
- [42] Massman W, Weil J. An analytical one-dimensional second-order closure model of turbulence statistics and the Lagrangian time scale within and above plant canopies of arbitrary structure. *Bound-Lay Meteorol* 1999;91:81–107.
- [43] Katul G, Chang W. Principal length scales in second-order closure models for canopy turbulence. *J Appl Meteorol* 1999;38:1631–43.
- [44] Sanz C. A note on k -epsilon modelling of vegetation canopy airflows. *Bound-Lay Meteorol* 2003;108:191–7.
- [45] Lumley J. Some comments on turbulence. *Phys Fluid A-Fluid Dyn* 1992;4:203–11.